Long-Term Effects of Sildenafil in a Rat Model of Chronic Mitral Regurgitation : Benefits of Ventricular Remodeling and Exercise Capacity

Kyung-Hee Kim, Yong-Jin Kim, Jung-Hun Ohn, Jimin Yang, Sang-Eun Lee, Sae-Won Lee, Hyung-Kwan Kim, Jeong-Wook Seo and Dae-Won Sohn

Circulation. 2012;125:1390-1401; originally published online February 8, 2012;
doi: 10.1161/CIRCULATIONAHA.111.065300
Circulation is published by the American Heart Association, 7272 Greenville Avenue, Dallas, TX 75231

Print ISSN: 0009-7322. Online ISSN: 1524-4539

Long-Term Effects of Sildenafil in a Rat Model of Chronic Mitral Regurgitation

Benefits of Ventricular Remodeling and Exercise Capacity

Kyung-Hee Kim, MD; Yong-Jin Kim, MD; Jung-Hun Ohn, MD; Jimin Yang, MA; Sang-Eun Lee, MD; Sae-Won Lee, PhD; Hyung-Kwan Kim, MD; Jeong-Wook Seo, MD; Dae-Won Sohn, MD

Background—We tested the hypothesis that chronic treatment with sildenafil attenuates left ventricular (LV) remodeling and prevents exercise intolerance in chronic mitral regurgitation (MR).

Methods and Results—MR was created in Sprague-Dawley rats by making a hole on the mitral leaflet. Two weeks after MR creation, MR and LV dilatation were confirmed by echocardiography, and rats were randomly assigned to sildenafil treatment (MR+sildenafil group; 50 mg/kg PO twice a day; n=16) or normal saline only (MR group; n=16) and continued for 4 months. Sixteen sham rats were compared with MR rats. After 4 months, LV size was smaller in the MR+sildenafil compared with the MR group (LV end-systolic dimension, 4.7±0.3 for sham versus 5.9±0.3 for MR+sildenafil versus 7.4±0.5 mm for MR; $P<0.05$; LV end-diastolic dimension, 8.3±0.4 versus 10.5±0.2 versus 11.7±0.61 mm, respectively; $P<0.05$). LV ejection fraction was greater in the MR+sildenafil group than in the MR group (70.2±2.2% for sham versus 67.0±4.2% for MR+sildenafil versus 58.9±2.5% for MR; $P=0.01$). Serial treadmill test revealed that exercise capacity was reduced in the MR but not in the MR+sildenafil group. Transcriptional profiling of cardiac apical tissues revealed that gene sets related to inflammatory response, DNA damage response, cell cycle checkpoint, and cellular signaling pathways were significantly enriched by genes with reciprocal changes. Pathological analysis showed that perivascular fibrosis was more prominent in the MR than in the MR+sildenafil group and that the percentage of terminal deoxynucleotidyl transferase–mediated dUTP nick-end labeling–positive cells was 2-fold greater in the MR compared with the MR+sildenafil group.

Conclusions—Sildenafil significantly attenuates LV remodeling and prevents exercise intolerance in a rat model of chronic MR. This benefit may be associated with the antiapoptotic, anti-inflammatory effects of sildenafil. **(*Circulation*. 2012; 125:1390-1401.)**

Key Words: exercise capacity ■ left ventricular remodeling ■ microarrays ■ mitral regurgitation ■ sildenafil

Mitral regurgitation (MR) is a growing clinical problem as the mean age of the population advances.[1,2] Currently, effective medical therapy is not available to prevent left ventricular (LV) remodeling and deterioration of exercise capacity and thus delay the need for surgery. Although vasodilator therapy is effective in acute MR,[3] its benefit is not established in chronic MR.[4,5]

Editorial see p 1341
Clinical Perspective on p 1401

Sildenafil citrate is a selective inhibitor of phosphodiesterase-5, which catalyzes the breakdown of cGMP, one of the primary factors causing smooth muscle relaxation. By its potent action of enhancing NO-driven cGMP accumulation and ensuing vasodilation, sildenafil is widely used for the treatment of erectile dysfunction. However, growing evidence supports that inhibition of phosphodiesterase-5 may have important antihypertrophic, antiapoptotic, and ischemic preconditioning effects that may limit myocardial remodeling in response to stress and attenuate the substrate for heart failure development. In murine models of myocardial pressure overload, inhibition of phosphodiesterase-5 was associated with inhibition of myocyte hypertrophy and interstitial fibrosis, preservation of cardiac function, and deactivation of various hypertrophy signaling cascades.[6–8] Phosphodiesterase-5 inhibition also promotes opening of mitochondrial K-ATP channels, a

Received September 2, 2011; accepted January 23, 2012.

From the Departments of Internal Medicine, Cardiovascular Center (K.K., Y.K., J.Y., Sang-Eun Lee, Sae-Won Lee, H.K., D.S.); Internal Medicine, Division of Endocrinology and Metabolism (J.O.); and Department of Pathology (J.S.), Seoul National University College of Medicine, Seoul National University Hospital, Seoul, Korea.

The online-only Data Supplement is available with this article at http://circ.ahajournals.org/lookup/suppl/doi:10.1161/CIRCULATIONAHA.111.065300/-/DC1.

Correspondence to Yong-Jin Kim, MD, PhD, Seoul National University College of Medicine, Cardiovascular Center, Seoul National University Hospital, 101 Daehak-ro, Jongno-gu, Seoul 110–744, Republic of Korea. E-mail kimdamas@snu.ac.kr

Circulation **is available at http://circ.ahajournals.org** **DOI: 10.1161/CIRCULATIONAHA.111.065300**

putative target of reactive oxygen species generated in response to both ischemia/reperfusion and doxorubicin treatment, and reduces doxorubicin or ischemia/reperfusion-induced apoptosis.[9,10] Additionally, clinical studies of sildenafil in patients with heart failure have reported improved exercise capacity coupled with reduced pulmonary vascular resistance and better endothelial function.[11,12]

Accordingly, we hypothesized that sildenafil may have a beneficial effect in chronic MR because the process of LV remodeling shares some of the aforementioned molecular mechanisms in chronic MR. In the present study, we evaluated the long-term effect of sildenafil on survival, myocardial function, remodeling, and exercise capacity using a rat model of chronic MR. Additionally, we investigated potential mechanisms for the beneficial effects of sildenafil using cDNA microarray technology.

Methods

Animal Handling

Male Sprague-Dawley rats (n=52) with an initial weight of 350 to 400 g were used. The rats were given free access to tap water and standard rat chow and housed in a room with a 12/12-hour light cycle, a temperature of 21°C, and a humidity of 55%. The experimental protocols were approved by the Institutional Animal Care and Use Committee of Seoul National University Hospital.

Creation of MR Model and Study Design

Surgical creation of MR was performed under the guidance of transesophageal echocardiography in 11-week-old rats.[13,14] We used intracardiac echocardiographic catheters (Acuson/Siemens Corp, Mountain View, CA) for transesophageal studies. After the insertion of an echocardiographic catheter into the esophagus, left thoracotomy was performed through the fourth or fifth intercostal space. A needle (0.5-mm external diameter) was inserted into the LV via apical puncture. After we found the needle tip under the echocardiographic image, we advanced the needle toward the anterior mitral valve to puncture the leaflets and create MR (detailed methodology is described in the online-only Data Supplement). MR was considered significant if a regurgitant jet area was >45% of the left atrium.[14] Sham animals underwent the same procedures except for mitral leaflet injury.

Two weeks after the surgery, we confirmed the development of MR with LV dilation, and the rats were randomly assigned to sildenafil treatment (MR+sildenafil group; 50 mg/kg PO twice a day; n=16) or normal saline only (MR group; n=16) (Table 1). An oral dose of 100 mg/kg per day of sildenafil (Viagra, Pfizer) was administered orally by gavage twice a day on the basis of previous studies showing a pleiotropic vascular effect in a heart failure model.[15–17] Sixteen sham rats were compared with MR rats.

We started the treatment 2 weeks after MR creation and continued for 14 weeks according to the results of our pilot study,[13] as follows: (1) Ejection fraction (EF) remained in the normal range despite progressive increase of LV size; (2) no additional death occurred during this period (see the online-only Data Supplement for details). Cardiac function and exercise capacity were monitored every 2 or 4 weeks. At the end of the 14-week treatment, pressure-volume analysis was performed, and the hearts and lungs were harvested for tissue determinations. The detailed experimental protocol is shown in Figure 1.

Survival Analysis

We examined the effects of sildenafil on the survival of MR rats. The day of oral administration of sildenafil was defined as day 0. This survival analysis covered the entire experimental period to day 100.

Table 1. General and Echocardiographic Characteristics 2 Weeks After Mitral Regurgitation (13 Weeks of Age)

Variables	Sham Group (n=16)	MR Group	
		MR (n=16)	MR+Sildenafil (n=16)
Body weight, g	437.0±8.8	422.8±8.8	423.8±10.4
Systolic BP, mm Hg	130.5±12.9	133.2±6.5	128.4±8.2
Diastolic BP, mm Hg	93.6±15.1	95.7±14.4	90.1±10.1
HR, bpm	350±18.1	354±14.9	347±22.4
HR, bpm*	312.8±17.3	318.3±15.7	315.3±18.7
EF,%	70.4±0.94	78.5±1.0†	78.7±1.54†
EDD, mm	7.76±0.2	9.01±0.44†	9.01±0.48†
ESD, mm	4.21±0.19	4.15±0.19	4.11±0.22
SWT, mm	1.32±0.04	1.1±0.05†	1.09±0.06†
PWT, mm	1.35±0.01	1.07±0.06†	1.08±0.07†
E velocity	65.2±7.1	106.1±12.1	104.1±16.9
LV mass, g	683±14.44	695±15.7	697.7±14.3
LV mass index, mg/g*	1.60±0.04	1.65±0.06	1.62±0.05

Data are mean±SEM. MR indicates mitral regurgitation; BP, blood pressure; HR, heart rate; EF, ejection fraction; EDD, end-diastolic dimension; ESD, end-systolic dimension; SWT, end-diastolic wall thickness of interventricular septum; PWT, end-diastolic wall thickness of posterior wall; E velocity, mitral inflow E velocity (cm/s); and LV, left ventricular.

*Heart rate and LV mass were estimated in vivo by echocardiography.

†$P<0.05$ for difference from control.

Physiological Study

Echocardiography

Transthoracic echocardiography was performed 1 week before and 2, 4, 6, 9, 12, and 16 weeks after the creation of MR on spontaneously breathing rats placed in the dorsal recumbent position. Rats were lightly sedated with inhalation of the lowest possible dose of isoflurane (initially 4%, then ≈2% to 3%) mixed with oxygen. Images were acquired with a 9-MHz transducer connected to a Toshiba echocardiography machine (Nemio, Toshiba Co, Tokyo, Japan). LV septal and posterior wall thickness (SWT and PWT) and LV end-diastolic/systolic dimension (EDD/ESD) were measured with M-mode echocardiography at the papillary muscle level. LVEF was calculated as $(LVEDD^2-LVESD^2)/LVEDD^2$. LV mass was estimated by a formula validated in small animals[18] and adjusted for body weight: LV mass=$([SWT+PWT+LVEDD]^3-LVEDD^3)\times 1.04$.

Color Doppler mapping of MR jets was used to semiquantitatively assess the severity of MR.[19] MR jet areas and LA areas were measured in the apical long-axis view, and the ratio of MR jet area to LA areas was calculated (Figure ID in the online-only Data Supplement). Early diastolic transmitral flow (E velocity) was measured in the apical 4-chamber view with a 1.5 mm–sized sample volume placed at the tips of the mitral leaflets. All parameters were evaluated on an average of 5 consecutive beats. A single echocardiographer experienced in >500 cases of rat echocardiography performed all data acquisition.

Exercise Test and Blood Pressure Monitoring

Maximal exercise capacity was evaluated with a Rota Rod treadmill (Ugo Basile, Comerio, Italy), in which rats run on a knurled drum as the drum rotates to avoid falling off. Animals were trained twice before the test to adjust the treadmill more familiarly. Treadmill speed was gradually increased from 3 to 15 rpm every 1 minute. Exercise time was recorded. The observer blinded to the study group recorded episodes of the immobility response as a result of exhaustion.

Systolic and diastolic blood pressures were measured in conscious rats via the tail-cuff method (Biopac System Inc) at 1 week before

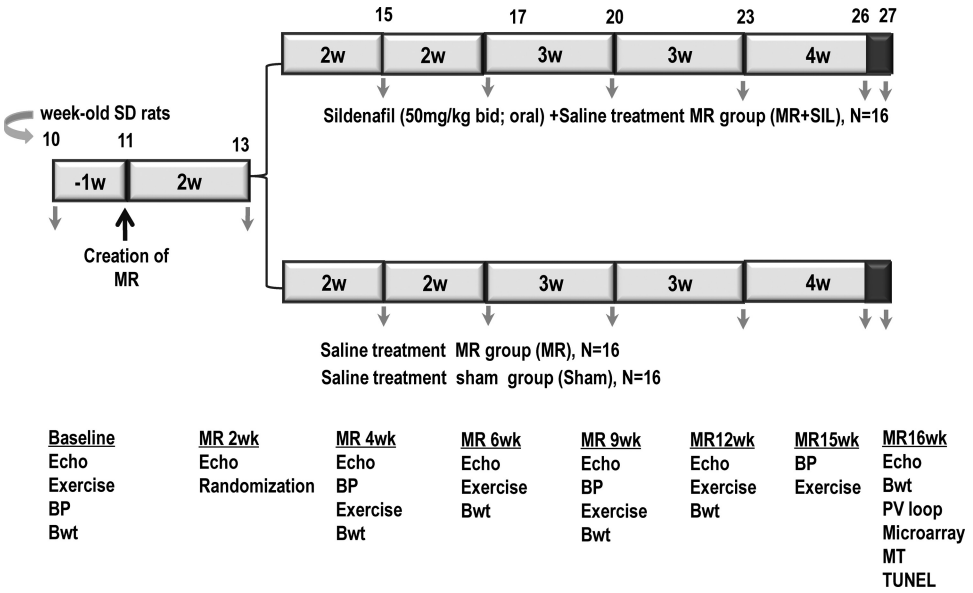

Figure 1. Schematic illustration of experimental protocol. SD indicates Sprague-Dawley; MR, mitral regurgitation; SIL, sildenafil; echo, echocardiography; BP, blood pressure; Bwt, body weight; PV, pressure-volume; and TUNEL, terminal deoxynucleotidyl transferase–mediated UTP nick-end labeling.

and 2, 4, 9, and 15 weeks after the creation of MR. At least a 1-day interval was given for the blood pressure measurements after the echocardiographic examination or exercise test to minimize stress on the animals.

Invasive Hemodynamic Measurements

At 16 weeks after MR creation, invasive hemodynamic measurements were obtained with the use of a 1.4F high-fidelity Millar pressure catheter, as described previously (see detailed Methods in the online-only Data Supplement).[20,21]

Histopathological Analysis

After hemodynamic measurements were performed, the rats were euthanized, the hearts and lungs were harvested and weighed, and the apical scar was excluded.

RNA Isolation

Fresh LV apex, excluding the apical scar, was immediately stored in RNAlater (Ambion/Applied Biosciences, Streetsville, Ontario, Canada) at −80°C until use. The hearts were homogenized in TRIzol reagent (Invitrogen, Burlington, Ontario, Canada), and total RNA was isolated according to the manufacturer's instructions. RNA was further purified to remove genomic DNA contamination and was concentrated with the use of an RNeasy Plus Mini kit (Qiagen, Mississauga, Ontario, Canada). Samples with optical density ratio 260/280 >1.8, 28S/18S >1.6 with the use of a Bioanalyzer 2100 (Agilent, Santa Clara, CA) were selected for microarray processing.

Microarray Analysis

Apical heart RNA excluding scar tissue was labeled with either cyanine 3-CTP (Cy3) or cyanine 5-CTP (Cy5) (PerkinElmer, Boston, MA) with the use of the Low RNA Input Fluorescent Linear Amplification Kit (Agilent Technologies) and hybridized onto an Agilent whole rat genome array (G4131A). RNA samples from 3 rats in each group were pooled and hybridized onto 1 chip. The arrays were scanned at 2 different intensities, and the images were analyzed for background correction. Both BMP4 and FGF2 samples were cohybridized with RNA from the starting point, and a dye swap was performed. The arrays were normalized, and the differential gene expression was analyzed by the R and bioconductor-based method LIMMA (detailed in Methods in the online-only Data Supplement).

We performed gene set enrichment analysis to find molecular pathways or gene ontologies that are made up of differentially expressed genes in each biological condition.[22] Difference in mean log-transformed intensity for each experimental group was used as a metric for sorting probes in gene set enrichment analysis. After genes were sorted according to the metric, enrichment scores were assigned to 2394 different gene sets curated in the mSigDB database (http://www.broadinstitute.org/gsea/msigdb/). Gene sets with high absolute values of enrichment score are molecular pathways or gene ontologies that are made up of upregulated or downregulated genes and are differentially regulated pathways. *P* values for the enrichment scores were calculated after permuting class labels of each experimental condition, and gene sets with *P* values <0.05 were extracted. Gene sets with absolute enrichment score >0.35 and *P* value <0.05 were visualized as a network with nodes representing gene sets and edges connecting 2 nodes if hypergeometric *P* value for testing the significance of gene overlap is within 1 percentile of the whole *P* values.[23]

Verification of Gene Expression With Reverse Transcription Polymerase Chain Reaction

Total RNA was isolated with the use of an RNeasyPlus Mini Kit (Qiagen), and cDNA was synthesized with the use of the PrimeScript First-Strand cDNA Synthesis Kit (Takara) with 1 μg of each total RNA sample according to the manufacturer's instruction. cDNA (1 μL) was amplified by polymerase chain reaction with the use of the TaKaRa Ex Taq Kit (Takara) with specific primers (Table 2). GAPDH was chosen as an endogenous control. Quantification of band intensity was analyzed with the use of TINA 2.0 (RayTest) and normalized to the intensity of GAPDH.

Immunohistochemical Analysis

See the online-only Data Supplement for details. Mid ventricles were removed for histopathology and were preserved in 4% paraformaldehyde and embedded in paraffin. The tissue was sectioned into 4-μm sections and stained with Masson trichrome for evaluation of the degree of fibrosis and with picrosirius red for measurement of collagen deposition. Apoptosis was assessed with the use of the terminal deoxynucleotidyl transferase–mediated UTP nick-end labeling (TUNEL) technique (DNA fragmentation; Oncor, Gaithersburg, MD). The detailed protocol was published previously.[24]

Table 2. Primer Sequences for Validating Microarray by Real-Time Polymerase Chain Reaction

Gene Name	Forward Primer	Reverse Primer	Gene Bank ID
IL6	TCTCGAGCCCACCAGGAACGAAA	GTAGGGAAGGCAGTGGCTGTCA	NM_012589
IL18	ATCCTAGCTGCCTGCTCCAGCTG	CTGGTCTGGGATTCGTTGGCTGT	AY077842
CDKN2a	CTCTCCCGACCGGTGCACGA	TAGGCACCTGGGCGTGCTTG	NM_031550
NOS2	ACTCCATCGACCCGCCCACA	GCAGTGCTACAGCTCCGGGC	NM_012611
NOS3	TGCCTTTGCTCGAGCGGTGG	CTCCACTAGGCCAGGCCGGT	NM_012589
GAPDH	CAAATTCGTTGTCATACCAG	CGTGGAAGGACTCATGAC	NM_017008.3

IL indicates interleukin; NOS, NO synthase.

Statistical Analysis

Data are presented as mean±SEM. The normality of all parameters was tested with the Kolmogorov-Smirnov test. The differences among groups were compared by unpaired *t* test or 1-way ANOVA, followed by the Bonferroni test. In cases in which normality was excluded, the nonparametric Kruskal-Wallis H test was performed, and the Mann–Whitney *U* test was used for post hoc analysis. Repeated-measures ANOVA was performed to analyze the changes of several variables over time such as LVEF, LV dimension, LV mass index, and exercise capacity. Survival data were evaluated by the Kaplan–Meier method with pairwise comparison conducted with the log-rank test. All statistical analyses were performed with the use of SPSS 17.0 version (SPSS Inc, Chicago, IL), and P values <0.05 were considered statistically significant.

Results

Survival Analysis

A total of 52 rats were used in this study. After surgery, 2 rats died of bleeding, and 2 rats died in the acute stage within 2 weeks after MR operation as a result of pulmonary edema and unknown cause. Three of 16 rats in the MR group died during the study period. However, no deaths were noted in the MR+sildenafil and sham groups. A Kaplan–Meier survival curve showed the comparison between MR+sildenafil and MR rats ($P=0.07$; Figure 2A).

Hemodynamic Study

LV Remodeling After MR Creation

Mean MR jet area was 15±3 mm^2, and the mean ratio of MR jet area to LA area was 56±8% at 2 weeks after the operation. There was no MR in the sham group. Mitral E velocity increased at 2 weeks (65.2±7.1 versus 105.1±15.1 cm/s; $P<0.05$) in the MR groups, whereas it did not change in the sham group (66.4±6.4 versus 64.5±5.5 cm/s; $P=0.76$). Figure 3 demonstrates the time-dependent changes in LV diameter, EF, and LV mass index. Baseline examinations showed no difference in LV diameters among the 3 groups (LVESD, 4.0±0.1 versus 4.1±0.1 versus 4.1±0.1 mm;

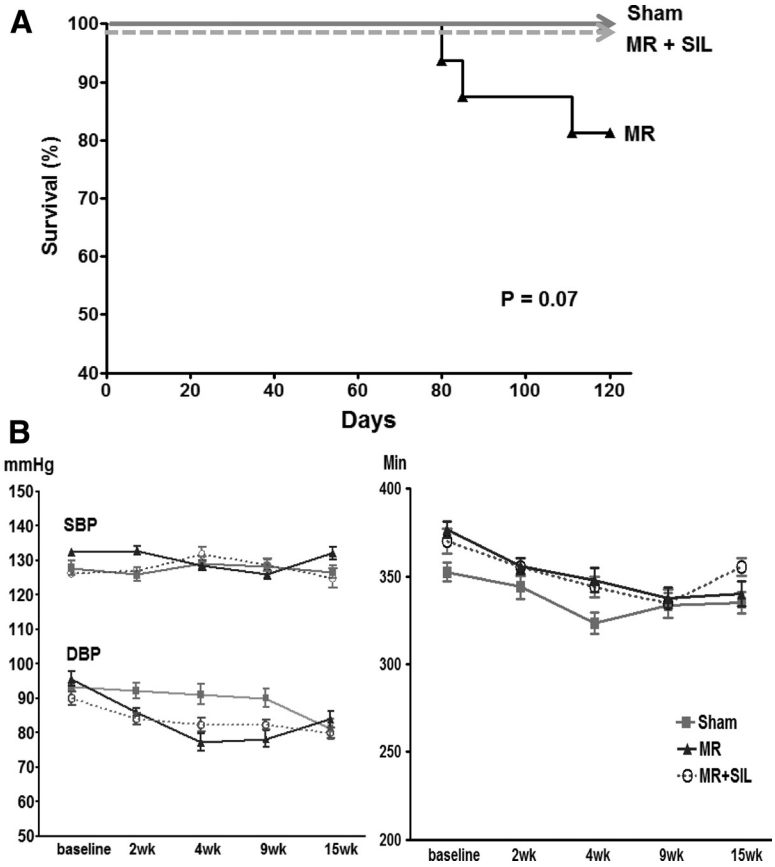

Figure 2. A, Survival analysis. Kaplan–Meier survival curve shows the comparison between mitral regurgitation (MR)+sildenafil (SIL) rats and MR rats ($P=0.07$). **B**, Serial changes in blood pressure and heart rate (HR). SBP indicates systolic blood pressure; DBP, diastolic blood pressure.

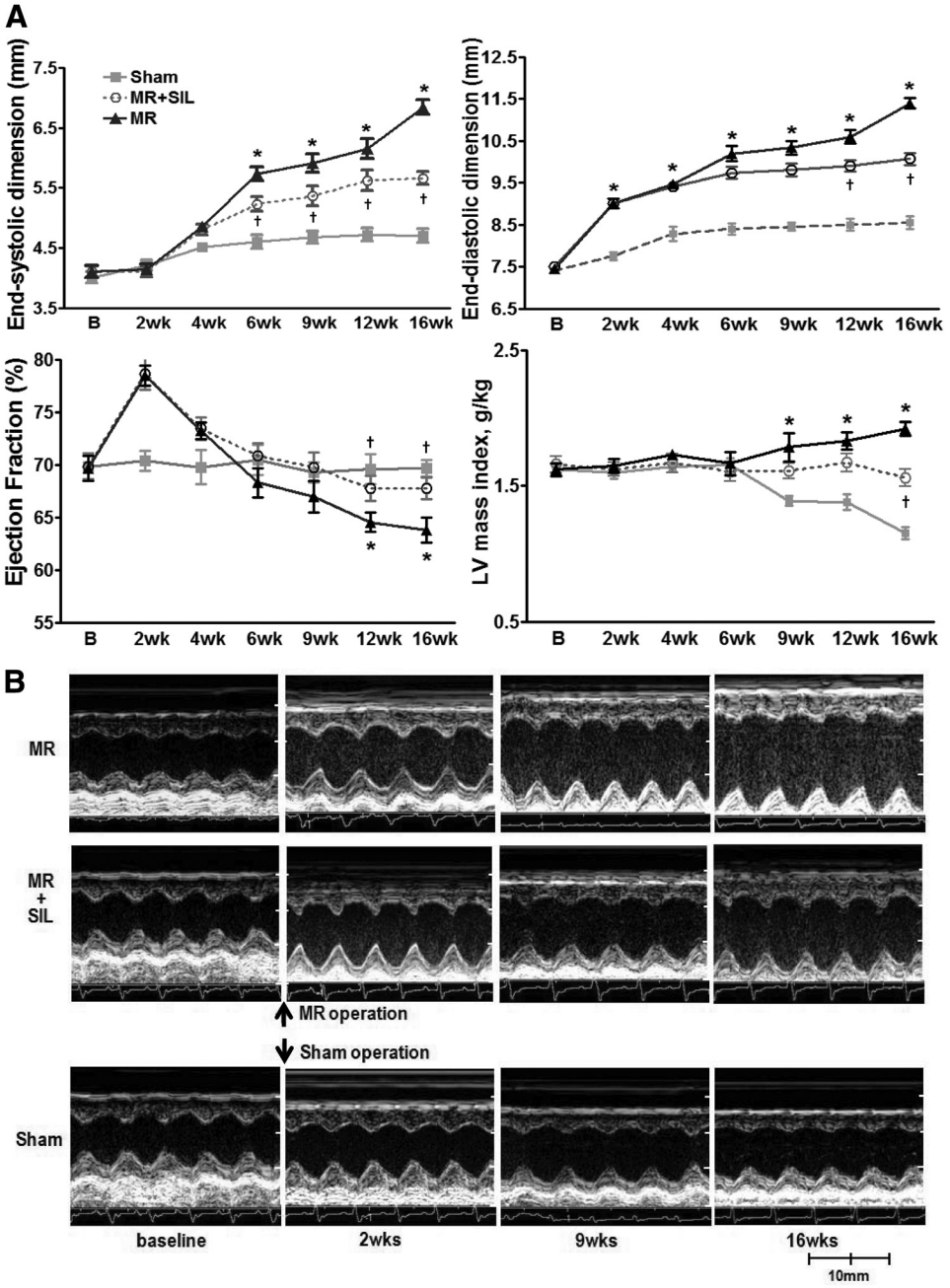

Figure 3. A, Serial changes in echocardiographic measurements. **B**, Representative M-mode echocardiograms from the 3 groups. MR indicates mitral regurgitation; SIL, sildenafil; LV, left ventricle; B, baseline; and wk, weeks after MR operation. *$P<0.05$ for difference from sham group; †$P<0.05$ for difference from MR group.

LVEDD, 7.4±0.1 versus 7.5±0.1 versus 7.5±0.1 mm for sham, MR, and MR+sildenafil groups, respectively; $P=0.82$). The LV started to dilate immediately after MR creation and showed progressive dilation until week 16. There was a significant difference in LVESD between the MR and MR+sildenafil groups from week 6, whereas LVEDD did not differ significantly until week 12. Consequently, LVEF started to decrease from week 6 in the MR group, whereas it was preserved until week 16 in the MR+sildenafil group. With increasing LVESD, death started to occur, as shown in the Kaplan–Meier curve (Figure 2A). Weight gain tended to lag behind that of the sham rats in the MR and MR+sildenafil rats, but this was without statistical significance (Figure II in the online-only Data Supplement). The LV mass index increased significantly in the MR group compared with the sham group (1.15±0.04 versus 1.71±0.05 mg/g; $P<0.05$). Sildenafil treatment attenuated the increase of LV mass index (11.7% reduction; $P=0.01$). There were no significant changes in blood pressure and heart rate among the groups (Figure 2B).

Exercise Capacity

There was no difference in exercise duration among the groups until week 6 after MR, when it became shorter in the MR group than in the sham group (720±15 for sham versus

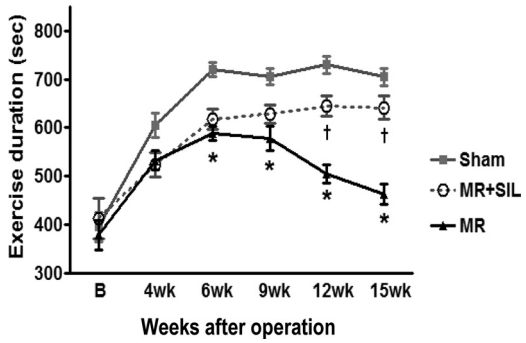

Figure 4. Comparison of exercise duration among the 3 groups. MR indicates mitral regurgitation; SIL, sildenafil; and B, baseline. *$P<0.05$ for difference from sham group; †$P<0.05$ for difference from MR group.

588±15 for MR versus 617±21 seconds for MR+sildenafil; $P<0.05$ for difference from sham versus MR; Figure 4). Thereafter, exercise capacity was impaired progressively in the MR group compared with the sham group (at week 15, 705±18 for sham versus 462±21 seconds for MR; $P<0.05$). However, exercise duration was maintained in the sildenafil-treated MR rats (641±14 seconds for MR+sildenafil; $P<0.05$ for difference from MR).

Invasive Hemodynamic Measurement

At week 16, rats underwent invasive hemodynamic assessment and were euthanized for pathological analysis (Table 3 and Figure 5). Heart rate, LV end-diastolic pressure, −dP/dt, and the end-diastolic pressure-volume relation were not different among the groups. However, end-systolic volume, end-diastolic volume, and stroke volume were greater in the MR group than in the sham group. The end-systolic pressure-volume relation, +dP/dt, preload recruitable stroke work, and EF were significantly decreased in the MR group, indicating contractile dysfunction. Sildenafil treatment prevented systolic functional impairment in the MR+sildenafil group compared with the MR group, as follows: EF, +28% ($P<0.05$); end-systolic pressure-volume relation, +116% ($P<0.05$); and preload recruitable stroke work, +30% ($P<0.05$).

Table 3. Hemodynamic Parameters 16 Weeks After Mitral Regurgitation (27 Weeks of Age)

		MR Group	
Variables	Sham Group (n=16)	MR (n=13)	MR+Sildenafil (n=16)
Body weight, mg	614.0±10.0	587.1±10.2	594.2±5.7
Lung, g	1.08±0.15	1.46±0.20*	1.23±0.17*†
Lung/body weight, mg/g	1.75±0.24	2.48±0.31*	2.07±0.27*†
HR, bpm	321.5±20.1	322.7±24.7	325.4±22.8
ESV, μL	127.2±5.9	443.5±25.4*	321.2±37.4*†
EDV, μL	430.9±27.6	1113.6±61.9*	998.7±54.7*†
Ejection fraction, %	70.2±1.4	60.7±3.5*	67.2±3.7
Stroke volume, μL	303.1±21.0	670.4±35.8*	677.5±48.5*
LVESP, mm Hg	101.3±7.5	105.4±6.3	106.4±4.0
LVEDP, mm Hg	10.5±3.5	12.3±2.3	11.2±2.1
+dP/dt, mm Hg/s	5124±228	4367±315*	4527±204
−dP/dt, mm Hg/s	−3781±366	−3543±312	−3431±311
ESPVR, mm Hg/μL	0.324±0.102	0.121±0.010*	0.262±0.031†
EDPVR, mm Hg/μL	0.010±0.002	0.013±0.001	0.011±0.003
PRSW, mm Hg	111.1±24.5	68.7±14.2*	89.3±10.1†

Data are mean±SEM. MR indicates mitral regurgitation; HR, heart rate; ESV, end-systolic volume; EDV, end-diastolic volume; LVESP, left ventricular end-systolic pressure; LVEDP, left ventricular end-diastolic pressure; ESPVR, end-systolic pressure-volume relationship; EDPVR, end-diastolic pressure-volume relationship; and PRSW, preload recruitable stroke work.

*$P<0.05$ for difference from control.

†$P<0.05$ for difference from MR.

Microarray Analysis

A total of 448 genes were differentially expressed by at least 1.5-fold in MR rats ($P<0.05$), including 197 upregulated and 251 downregulated genes compared with the sham or the MR+sildenafil group. The heat map in Figure III in the online-only Data Supplement demonstrates a consistent pattern of change of these genes in each condition. Table I in the online-only Data Supplement lists genes well established in the pathophysiology of cardiovascular disease that were upregulated >1.5-fold in the MR group and downregulated in the MR+sildenafil group.

For biological interpretation, we performed gene set enrichment analysis (see Methods for details) to explore the transcriptional changes at the level of molecular pathways or gene ontologies. Figure 6A and 6B is the network representation of gene sets that are enriched with genes upregulated in MR and reciprocally downregulated after treatment with sildenafil and presumed to be primarily associated with the pharmacological effect of sildenafil in MR. It is notable that gene sets form several tightly interconnected structures or clusters that we can annotate with inflammatory response, DNA damage response, cell cycle checkpoint, and cellular signaling pathways associated with LV remodeling.

To confirm the changes in transcription level, we selected 5 representative genes implicated in DNA damage response, inflammatory response, endothelial function, and vascular remodeling: CDKN2A, interleukin-6, interleukin-18, endothelial NO synthase, and inducible NO synthase.[26,27] Real-time polymerase chain reaction demonstrated the validity of DNA microarray (Figure 6C and 6D).

With the transcriptional profiling study, it is suggested that the chronic hemodynamic stress induced by MR may activate stress response pathways such as inflammatory pathways, DNA damage response pathways, and cell cycle checkpoint pathways, leading to cell fate decisions such as apoptosis and LV remodeling. With attenuation of hemodynamic stress by treatment with sildenafil, the activated stress response pathways are moderated, suggesting that the 3 clusters of pathways provide the basis for the molecular and cellular mechanisms of the pathological changes in hearts undergoing chronic volume and pressure overload from MR.

Histopathological Analysis With Cardiac Fibrosis and Apoptosis

Gross pathological examination showed that the heart was significantly enlarged with eccentric hypertrophy in the MR group at week 16 (Figure 7A). However, hypertrophy was

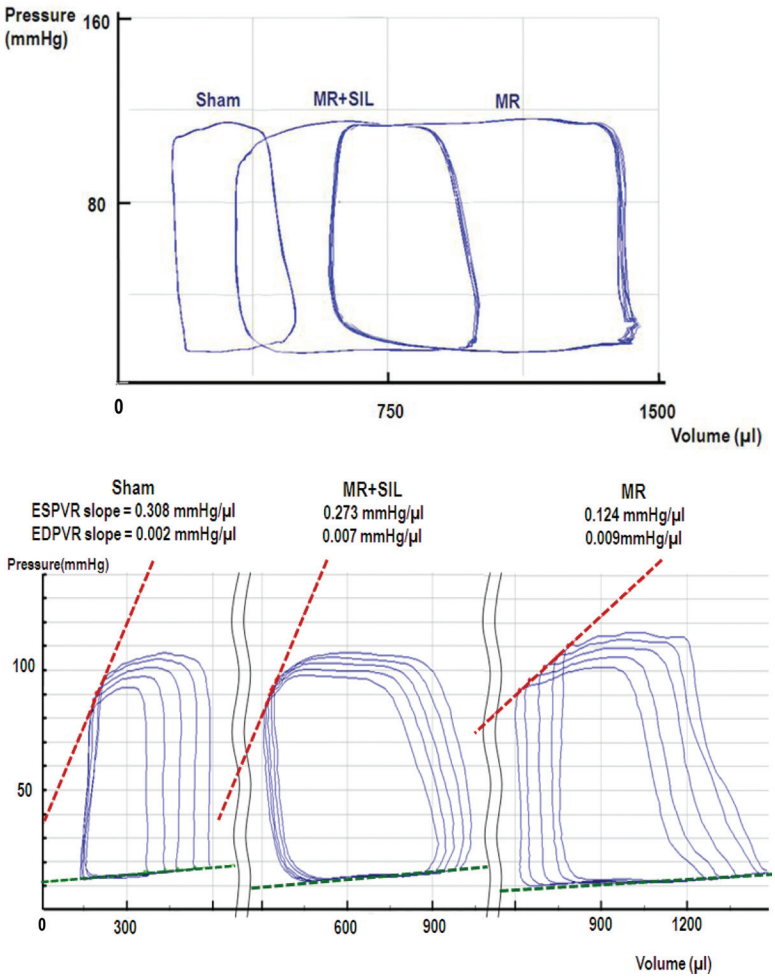

Figure 5. Representative pressure-volume loops from the 3 groups. Mitral regurgitation (MR)+sildenafil (SIL) group showed smaller left ventricular volume and greater end-systolic pressure-volume relation (ESPVR) (dotted line) compared with the MR group. EDPVR indicates end-diastolic pressure-volume relation.

reduced in sildenafil-treated MR rats. We found no difference in interstitial fibrosis among the groups. However, the extent of perivascular fibrosis was significantly larger in the MR group than in the MR+sildenafil group (Figure 7C through 7F). TUNEL staining showed a significant increase of cardiac apoptosis in the MR group (0.24±0.3%; $P<0.05$; Figure 8). In contrast, a significant inhibition of apoptosis was evident in the MR+sildenafil group (0.05±0.02%), which was comparable to that in the sham group (0.03±0.04%).

Discussion

The purpose of this study was to evaluate the effect of chronic administration of sildenafil on cardiac remodeling, function, and exercise capacity in rats with chronic MR. The major finding of the present study was that sildenafil prevented LV remodeling and exercise intolerance caused by chronic experimental MR. To our knowledge, this is the first study that shows that sildenafil is efficacious in the treatment of MR-induced LV remodeling and cardiac dysfunction. Additionally, we proposed potential mechanisms related to the effect of sildenafil: inhibition of inflammation and apoptosis.

Medical Management in Chronic MR

MR induces chronic LV volume overload and leads to LV contractile dysfunction, heart failure, and, finally, death. Although surgical correction of MR, the only definitive cure, carries reasonably low mortality and morbidity risks, medical therapeutics have a role in many clinical situations such as in a patient population with greater surgical risk. This has become more relevant because the main etiology of MR has changed from rheumatic to degenerative valve disease,[25] and the prevalence of MR increases with age because operative mortality for elderly patients is still high.[26] However, there is currently no recommended pharmacological therapy for chronic MR. Despite previous efforts, medical therapies for chronic MR have produced disappointing and conflicting results.

Small-Animal Model of Chronic MR

Little is known about the molecular and cellular mechanisms of LV remodeling induced by volume overload partly because of the absence of a small-animal model. In their pioneering work, Pu et al[14] developed an MR rat model for the first time. We successfully established a small-animal model of chronic MR and verified the pathophysiological features of this model. We described the detailed time course of LV remodeling and the relationship between progressive LV dilatation and LV dysfunction. Immediately after MR creation, we observed a slight increase of LV diastolic dimension without a change of systolic dimension and thus hyperdynamic LV. In this stage, LV wall thinning occurred as the LV began to dilate. A chronic compensated stage could be

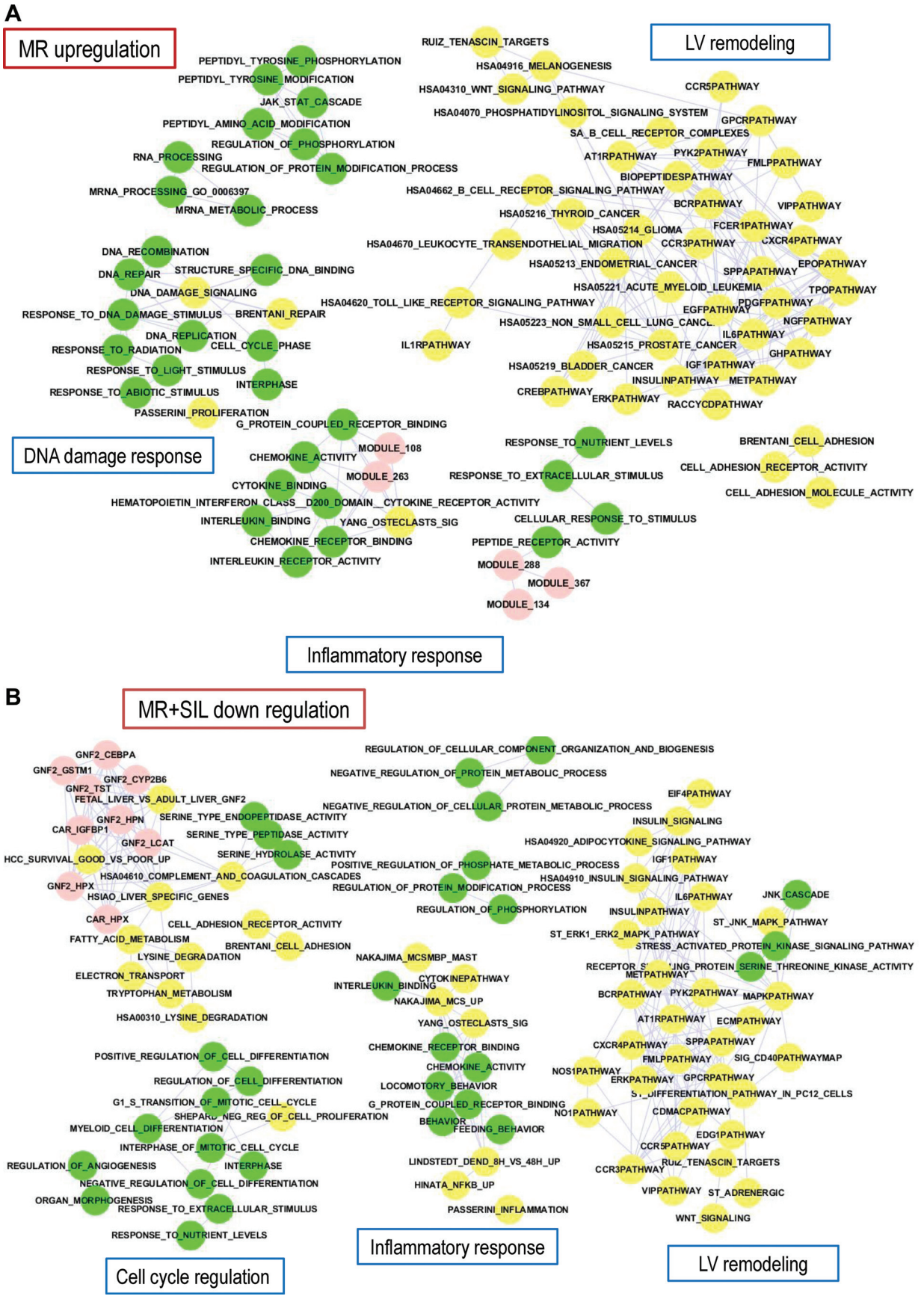

Figure 6. A and **B**, Network of gene sets with significant enrichment scores ($P<0.05$), made up of genes that are upregulated in the mitral regurgitation (MR) rat model. Nodes represent gene sets, and edges connect 2 nodes if the 2 gene sets share a significant

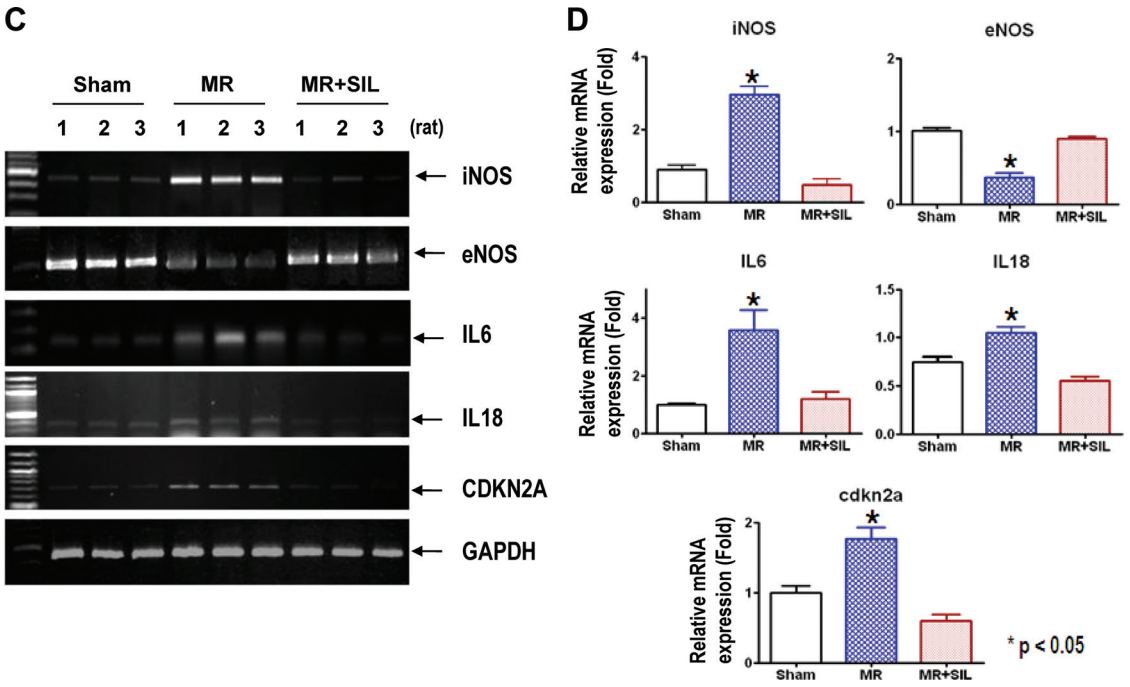

Figure 6 (Continued). number of genes in common by hypergeometric test (see Methods). Isolated nodes are omitted. Yellow nodes are gene ontology gene sets (C5), green nodes are curated gene sets from public pathway databases (C2), and pink nodes represent computational gene sets (C4). LV indicates left ventricular. **B**, Network of gene sets with significant enrichment scores ($P<0.05$), made up of genes that are downregulated after treatment with sildenafil in the MR rat model. SIL indicates sildenafil. **C**, mRNA regulation in the MR+SIL group. Real-time polymerase chain reaction of inducible NO synthase (iNOS), endothelial NO synthase (eNOS), interleukin (IL)-6, IL-18, and CDKN2A is shown (n=3 each). mRNA of factors for vascular remodeling, inflammation, and DNA damage was increased in the MR group but downregulated in the MR+SIL group. However, eNOS was downregulated in the MR group but increased in the MR+SIL group. **D**, Quantitative graph (n=3). *$P<0.05$ for difference from MR+SIL group.

defined from week 3 to approximately week 16. In this stage, LV diastolic and systolic volume increased progressively. Although it remained in the normal range, LVEF became significantly lower in the MR group from week 12. At week 16, load-independent contractile indices were significantly lower in the MR group, whereas diastolic parameters were not different. These results are consonant with several previous studies that demonstrated that MR is one of the few cardiac diseases in which diastolic function is supernormal.[27] Chronic adaptation to volume overload tends to decrease LV chamber stiffness and increase diastolic filling rates and dimension lengthening irrespective of systolic function in chronic MR.[28] Additionally, we did not find any increase of LV interstitial fibrosis in this stage of MR. Interstitial fibrosis is closely related to LV diastolic function.

Mechanism for LV Remodeling in MR

MR causes progressive LV dilation, wall thinning, and cardiomyocyte elongation, which recapitulates eccentric remodeling with inflammatory cell infiltration and extracellular matrix degradation. It has been suggested that inflammation and energy metabolism initiate cardiac remodeling.[29] Nemoto et al[30] showed that administration of the peroxisome proliferator-activated receptor-γ agonist rosiglitazone ameliorates MR-induced LV dysfunction accompanied by a decline in lipid content. Similarly, in the volume overload model of aortocaval fistula, upregulation of genes was related to inflammation, the extracellular matrix, the cell cycle, and apoptosis.[31] There was a 40-fold increase in the matricellular protein periostin, which inhibits connections between collagen and cells, thereby potentially mediating side-to-side slippage of cardiomyocytes and LV dilatation. These findings are consistent with our results that inflammation, the cell cycle, and DNA damage pathways that were upregulated in MR were prevented by sildenafil treatment.

Increased matrix metalloproteinase activity is associated with progressive LV dilatation and extracellular matrix degradation, contractile dysfunction, and neurohormonal activation in volume overload animal models. Zheng et al,[32] using a gene array analysis, reported recently that eccentric LV remodeling in isolated MR was associated with increased matrix metalloproteinase activity. However, we could not find a significant difference in matrix metalloproteinase families among the groups. This may imply that the relative contributions of each of these mechanisms change at different stages of remodeling. Extracellular matrix loss, inflammation, or bioenergetics dysfunction has been implicated at different time points in the pathophysiology of volume overload.[33]

Sildenafil for Treatment of MR

Emerging data indicate that phosphodiesterase-5 is present within cardiac myocytes and may play a role in modulating cGMP activity in various cardiac diseases.[34] Several observations from preclinical and short-term clinical studies support a role of sildenafil in the treatment of heart failure. In the present study, the anti-inflammatory and antiapoptotic effects of sildenafil seemed to play a key role in preventing LV remodeling.

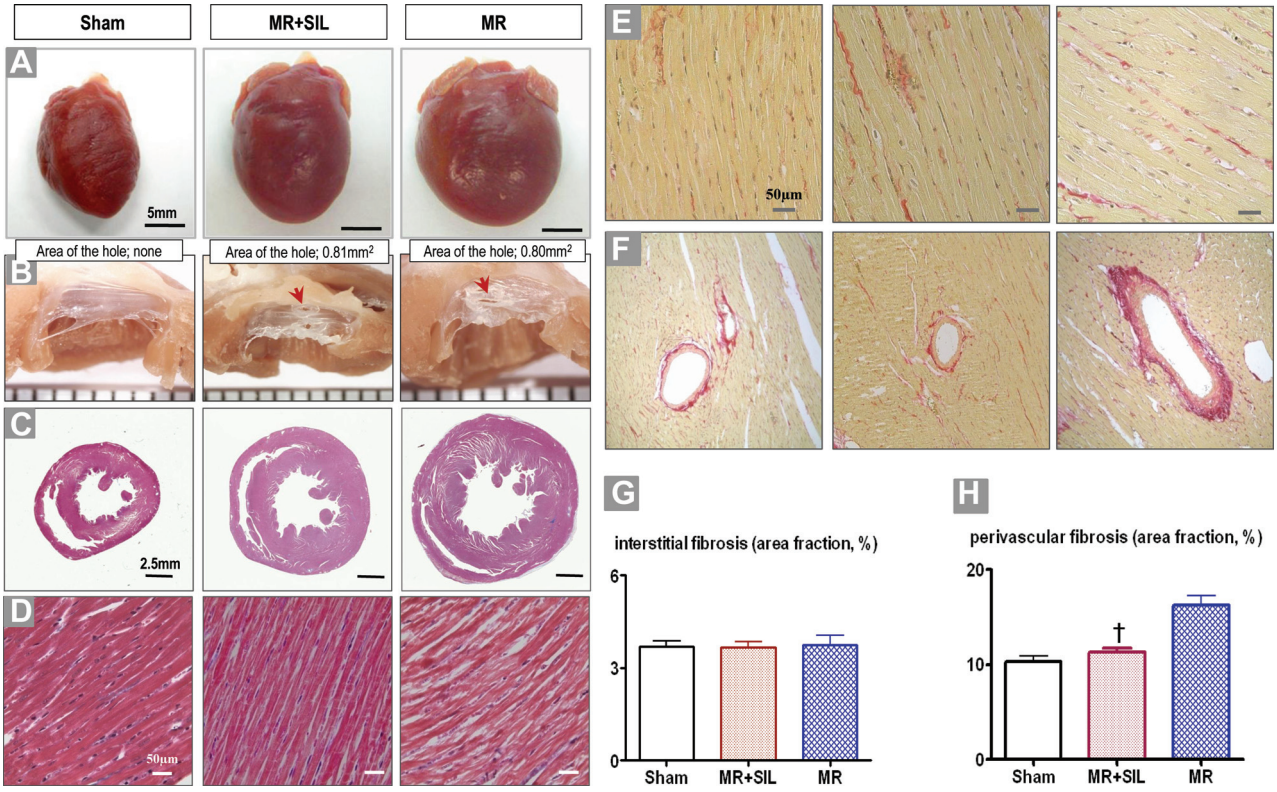

Figure 7. Comparison of pathological results. **A**, Eccentric hypertrophy was developed in the mitral regurgitation (MR) group. SIL indicates sildenafil. **B**, The hole created in the anterior leaflet of the mitral valve. **C**, **D**, **E**, **G**, Masson trichrome and picrosirius red staining showed no difference in interstitial fibrosis (**F** and **H**). The extent of perivascular fibrosis was significantly greater in the MR group than in the MR+SIL group († $P<0.05$ for difference from the MR group).

The endocardial perivascular area may represent an early fibrotic change in the MR model, probably because of relative endocardial ischemia due to the prolonged elevation of LV diastolic filling pressures. However, the extent of perivascular fibrosis was significantly smaller in the MR+sildenafil group than in the MR group. In recent years, there has been considerable interest in studying the effect of sildenafil on endothelial cell protection, which may trigger a signaling cascade (through the action of kinases including protein kinase C and other mitogen-activated protein kinases) and generation of NO by phosphorylation of endothelial NO synthase. An important property of sildenafil is its ability to increase endothelial NO synthase and inducible NO synthase proteins in the heart, and this has a direct cause-and-effect relationship in protection against myocardial infarction, as well as apoptosis in cardiomyocytes.[35,36] Because of the ability of sildenafil to augment NO synthase and cGMP levels, it is logical to hypothesize that cardiovascular dys-

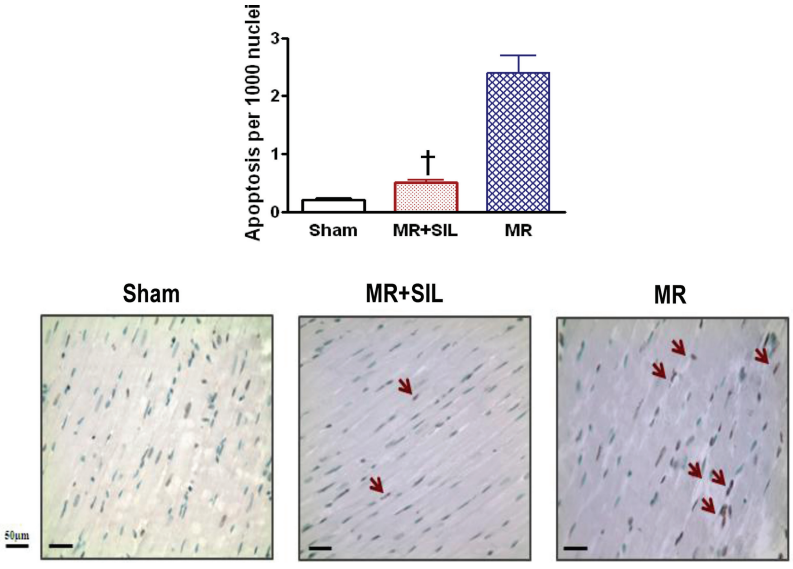

Figure 8. Representative apoptotic cells by terminal deoxynucleotidyl transferase–mediated UTP nick-end labeling analysis and quantitative apoptotic indices (†$P<0.05$ for difference from the mitral regurgitation [MR] group). Arrows indicate apoptotic cells. SIL indicates sildenafil.

function induced by chronic NO synthase inhibition would be alleviated by concomitant treatment with sildenafil.

Clinical and experimental data support a link between endothelial dysfunction and inflammation. Proinflammatory cytokines are increased in the myocardium as a response to stretch in MR patients and correlate with the extent of LV dilatation.[37] Inflammatory response and cytokine elaboration are integral components of the host response to tissue injury and play an active role in myocardial remodeling, and thus inflammatory mediators play a crucial role in the development of heart failure. Accordingly, several strategies to counterbalance the inflammatory response have been suggested. Possible targets involve proinflammatory and anti-inflammatory cytokines and their receptors, adhesion molecules, NO and NO synthase, reactive oxygen species, and different types of leukocytes. In this study, we demonstrated by microarray analysis that the inflammatory response was decreased in the sildenafil-treated group compared with MR rats.

Cell loss is another unifying feature found in nearly all forms of cardiomyopathies. Currently, the best-understood form of cell loss or cell death in heart failure is apoptosis. DNA fragmentation and cellular and nuclear shrinkage are 2 of the biochemical and morphological changes that classically characterize apoptosis. Barouch et al[38] demonstrated that cardiomyocyte apoptosis is associated with increased DNA damage and decreased survival in a murine model of obesity. In this study, we showed that the DNA damage pathway was upregulated in MR rats compared with sham and MR+sildenafil rats and that apoptotic cells were more prevalent in MR rats.

Nagayama et al[7,8] demonstrated that sildenafil treatment prevents further cardiac and myocyte dysfunction and progressive remodeling in an animal model of established hypertrophy caused by pressure overload. In the present study, we found a similar beneficial effect of sildenafil in an animal model of volume overload. The therapeutic effect of sildenafil has also been demonstrated in other animal models including an ischemia/reperfusion model and in anthracycline cardiomyopathy. These findings suggest that there is substantial overlap of molecular pathways in the development of different types of cardiac remodeling induced by various stimuli. In addition, these findings also suggest the multiple effects of sildenafil and cGMP.

Limitation of the Study

MR was created by making a hole in the mitral leaflet, and this MR model may not represent MR in humans, especially ischemic MR. This is an inherent limitation of the animal model of valve disease. However, our model is still useful to evaluate the effect of medical treatment on LV remodeling induced by MR. In this regard, the beneficial effect of sildenafil on volume overload–induced LV remodeling may have clinical implications. Further research is needed to delineate the exact mechanisms involved to allow for translation to the clinical setting.

Conclusion

Sildenafil attenuates LV remodeling and prevents exercise intolerance in a rat model of chronic MR. This benefit may be associated with the antiapoptotic, anti-inflammatory effects of sildenafil. Further research is needed to delineate the exact mechanisms involved and demonstrate the beneficial effects in patients with chronic MR.

Acknowledgments

The authors are grateful to Ha-Na Kim for her technical assistance. Sildenafil powder was kindly provided by Pfizer, Inc.

Sources of Funding

This study was supported by a grant from the Korea Institute of Medicine and the Korea Healthcare Technology Research and Development Project, Ministry for Health, Welfare, and Family Affairs, Republic of Korea (A090458 and A110092).

Disclosures

None.

References

1. Nkomo V, Gardin J, Skelton T, Gottdiener J, Scott C, Enriquez-Sarano M. Burden of valvular heart diseases: a population-based study. *Lancet*. 2006;368:1005–1011.
2. Iung B, Baron G, Butchart E, Delahaye F, Gohlke-Barwolf C, Levang O, Tornos P, Vanoverschelde J, Vermeer F, Boersma E. A prospective survey of patients with valvular heart disease in Europe: the Euro Heart Survey on Valvular Heart Disease. *Eur Heart J*. 2003;24:1231–1243.
3. Yoran C, Yellin E, Becker R, Gabbay S, Frater R, Sonnenblick E. Mechanism of reduction of mitral regurgitation with vasodilator therapy. *Am J Cardiol*. 1979;43:773–777.
4. Otto C. Evaluation and management of chronic mitral regurgitation. *N Engl J Med*. 2001;345:740–746.
5. Perry G, Wei C, Hankes G, Dillon S, Rynders P, Mukherjee R, Spinale F, Dell'Italia L. Angiotensin II receptor blockade does not improve left ventricular function and remodeling in subacute mitral regurgitation in the dog. *J Am Coll Cardiol*. 2002;39:1374–1379.
6. Takimoto E, Champion H, Li M, Belardi D, Ren S, Rodriguez E, Bedja D, Gabrielson K, Wang Y, Kass D. Chronic inhibition of cyclic GMP phosphodiesterase 5a prevents and reverses cardiac hypertrophy. *Nat Med*. 2005;11:214–222.
7. Nagayama T, Hsu S, Zhang M, Koitabashi N, Bedja D, Gabrielson K, Takimoto E, Kass D. Sildenafil stops progressive chamber, cellular, and molecular remodeling and improves calcium handling and function in hearts with pre-existing advanced hypertrophy caused by pressure overload. *J Am Coll Cardiol*. 2009;53:207–215.
8. Nagayama T, Hsu S, Zhang M, Koitabashi N, Bedja D, Gabrielson K, Takimoto E, Kass D. Pressure-overload magnitude-dependence of the anti-hypertrophic efficacy of PDE5a inhibition. *J Mol Cell Cardiol*. 2009;46:560–567.
9. Fisher P, Salloum F, Das A, Hyder H, Kukreja R. Phosphodiesterase-5 inhibition with sildenafil attenuates cardiomyocyte apoptosis and left ventricular dysfunction in a chronic model of doxorubicin cardiotoxicity. *Circulation*. 2005;111:1601–1610.
10. Salloum F, Abbate A, Das A, Houser J, Mudrick C, Qureshi I, Hoke N, Roy S, Brown W, Prabhakar S. Sildenafil (Viagra) attenuates ischemic cardiomyopathy and improves left ventricular function in mice. *Am J Physiol*. 2008;294:H1398–H1406.
11. Lewis G, Lachmann J, Camuso J, Lepore J, Shin J, Martinovic M, Systrom D, Bloch K, Semigran M. Sildenafil improves exercise hemodynamics and oxygen uptake in patients with systolic heart failure. *Circulation*. 2007;115:59–66.
12. Guazzi M, Samaja M, Arena R, Vicenzi M, Guazzi M. Long-term use of sildenafil in the therapeutic management of heart failure. *J Am Coll Cardiol*. 2007;50:2136–2144.
13. Kim K-H, Kim Y-J, Lee S-P, Kim H-K, Seo J-W, Sohn D-W, Oh B-H, Park Y-B. Survival, exercise capacity, and left ventricular remodeling in a rat model of chronic mitral regurgitation: serial echocardiography and pressure-volume analysis. *Korean Circ J*. 2011;41:603–611.
14. Pu M, Gao Z, Zhang X, Liao D, Pu DK, Brennan T, Davidson WR. Impact of mitral regurgitation on left ventricular anatomic and molecular remodeling and systolic function: implication for outcome. *Am J Physiol*. 2009;296:H1727–H1732.

15. Clozel M, Hess P, Rey M, Iglarz M, Binkert C, Qiu C. Bosentan, sildenafil, and their combination in the monocrotaline model of pulmonary hypertension in rats. *Exp Biol Med*. 2006;231:967–973.
16. Hassan M, Ketat A. Sildenafil citrate increases myocardial cGMP content in rat heart, decreases its hypertrophic response to isoproterenol and decreases myocardial leak of creatine kinase and troponin T. *BMC Pharmacol*. 2005;5:10.
17. Andersen A, Nielsen JM, Peters CD, Schou UK, Sloth E, Nielsen-Kudsk JE. Effects of phosphodiesterase-5 inhibition by sildenafil in the pressure overloaded right heart. *Eur J Heart Fail*. 2008;10:1158–1165.
18. Reffelmann T, Kloner RA. Transthoracic echocardiography in rats: evaluation of commonly used indices of left ventricular dimensions, contractile performance, and hypertrophy in a genetic model of hypertrophic heart failure (SHHF-Mcc-facp-rats) in comparison with Wistar rats during aging. *Basic Res Cardiol*. 2003;98:275–284.
19. Helmcke F, Nanda N, Hsiung M, Soto B, Adey C, Goyal R, Gatewood R Jr. Color Doppler assessment of mitral regurgitation with orthogonal planes. *Circulation*. 1987;75:175–183.
20. Lips DJ, van der Nagel T, Steendijk P, Palmen M, Janssen BJ, van Dantzig JM, de Windt LJ, Doevendans PA. Left ventricular pressure-volume measurements in mice: comparison of closed-chest versus open-chest approach. *Basic Res Cardiol*. 2004;99:351–359.
21. Pacher P, Nagayama T, Mukhopadhyay P, Bátkai S, Kass DA. Measurement of cardiac function using pressure-volume conductance catheter technique in mice and rats. *Nat Protocols*. 2008;3:1422–1434.
22. Subramanian A, Tamayo P, Mootha VK, Mukherjee S, Ebert BL, Gillette MA, Paulovich A, Pomeroy SL, Golub TR, Lander ES. Gene set enrichment analysis: a knowledge-based approach for interpreting genome-wide expression profiles. *Proc Natl Acad Sci U S A*. 2005;102:15545–15550.
23. Rivals I, Personnaz L, Taing L, Potier MC. Enrichment or depletion of a GO category within a class of genes: which test? *Bioinformatics*. 2007;23:401–407.
24. Loo DT. In situ detection of apoptosis by the TUNEL assay: an overview of techniques. *Methods Mol Biol.* 2011;682:3–13.
25. Ahmed MI, McGiffin DC, O'Rourke RA, Dell'Italia LJ. Mitral regurgitation. *Curr Prob Cardiol*. 2009;34:93–136.
26. DiGregorio V, Zehr KJ, Orszulak TA, Mullany CJ, Daly RC, Dearani JA, Schaff HV. Results of mitral surgery in octogenarians with isolated nonrheumatic mitral regurgitation. *Ann Thorac Surg*. 2004;78:807–813.
27. Zile MR, Tomita M, Nakano K, Mirsky I, Usher B, Lindroth J, Carabello B. Effects of left ventricular volume overload produced by mitral regurgitation on diastolic function. *Am J Physiol*. 1991;261:H1471–H1480.
28. Corin WJ, Murakami T, Monrad ES, Hess OM, Krayenbuehl HP. Left ventricular passive diastolic properties in chronic mitral regurgitation. *Circulation*. 1991;83:797–807.
29. Kai H, Kuwahara F, Tokuda K, Imaizumi T. Diastolic dysfunction in hypertensive hearts: roles of perivascular inflammation and reactive myocardial fibrosis. *Hypertension Res*. 2005;28:483–490.
30. Nemoto S, Razeghi P, Ishiyama M, De Freitas G, Taegtmeyer H, Carabello BA. PPAR-γ agonist rosiglitazone ameliorates ventricular dysfunction in experimental chronic mitral regurgitation. *Am J Physiol*. 2005;288:H77–H82.
31. Chen Y, Pat B, Gladden JD, Zheng J, Powell P, Wei CC, Cui X, Husain A, Dell'Italia LJ. Dynamic molecular and histopathological changes in the extracellular matrix and inflammation in the transition to heart failure in isolated volume overload. *Am J Physiol*. 2011;300:H2251–H2260.
32. Zheng J, Chen Y, Pat B, Dell'Italia LA, Tillson M, Dillon A, Powell PC, Shi K, Shah N, Denney T. Microarray identifies extensive downregulation of noncollagen extracellular matrix and profibrotic growth factor genes in chronic isolated mitral regurgitation in the dog. *Circulation*. 2009;119:2086–2095.
33. Hutchinson KR, Stewart JA, Lucchesi PA. Extracellular matrix remodeling during the progression of volume overload-induced heart failure. *J Mol Cell Cardiol*. 2010;48:564–569.
34. Senzaki H, Smith CJ, Juang GJ, Isoda T, Mayer SP, Ohler A, Paolocci N, Tomaselli GF, Hare JM, Kass DA. Cardiac phosphodiesterase 5 (cGMP-specific) modulates β-adrenergic signaling in vivo and is down-regulated in heart failure. *FASEB J*. 2001;15:1718–1726.
35. Das A, Xi L, Kukreja RC. Phosphodiesterase-5 inhibitor sildenafil preconditions adult cardiac myocytes against necrosis and apoptosis. *J Biol Chem*. 2005;280:12944–12955.
36. Sam F, Sawyer DB, Xie Z, Chang DLF, Ngoy S, Brenner DA, Siwik DA, Singh K, Apstein CS, Colucci WS. Mice lacking inducible nitric oxide synthase have improved left ventricular contractile function and reduced apoptotic cell death late after myocardial infarction. *Circ Res*. 2001;89:351–356.
37. Oral H, Sivasubramanian N, Dyke DB, Mehta RH, Grossman PM, Briesmiester K, Fay WP, Pagani FD, Bolling SF, Mann DL. Myocardial proinflammatory cytokine expression and left ventricular remodeling in patients with chronic mitral regurgitation. *Circulation*. 2003;107:831–837.
38. Barouch LA, Gao D, Chen L, Miller KL, Xu W, Phan AC, Kittleson MM, Minhas KM, Berkowitz DE, Wei C. Cardiac myocyte apoptosis is associated with increased DNA damage and decreased survival in murine models of obesity. *Circ Res*. 2006;98:119–124.

CLINICAL PERSPECTIVE

Mitral regurgitation (MR) induces chronic left ventricular volume overload and leads to left ventricular contractile dysfunction, heart failure, and, finally, death. Although surgical correction of MR, the only definitive cure, carries reasonably low mortality and morbidity risks, medical therapeutics have a role in many clinical situations such as in a patient population with greater surgical risk. However, there is currently no recommended pharmacological therapy for chronic MR. Despite previous efforts, medical therapies for chronic MR have produced disappointing and conflicting results. Since the early 2000s, sildenafil, part of a class of selective inhibitors of phosphodiesterase type 5, has been under intense study in various areas. Multiple lines of preclinical and clinical evidence support a therapeutic role for phosphodiesterase type 5 inhibition with sildenafil in the management of heart failure. Accordingly, we hypothesized that sildenafil may have a beneficial effect in chronic MR. The major findings of the present study are that sildenafil prevented left ventricular remodeling and exercise intolerance caused by chronic experimental MR. To our knowledge, this is the first study that shows that sildenafil is efficacious in the presence of MR. Additionally, we proposed potential mechanisms related to the effect of sildenafil: inhibition of inflammation and apoptosis. With consideration of the beneficial effects of sildenafil in MR rats, we can expect a therapeutic potential for sildenafil in patients with MR. Future clinical studies are needed.

ONLINE SUPPLEMENT

Long-Term Effects of Sildenafil in a Rat Model with Chronic Mitral Regurgitation; Benefits on ventricular remodeling and exercise capacity

Kyung-Hee Kim, MD[1]; Yong-Jin Kim, MD[1]; Jung-Hun Ohn, MD[2]; Sang-Eun Lee, MD[1]; Jimin Yang, MA[1]; Sae-Won Lee, PhD[1]; Hyung-Kwan Kim, MD[1]; Jeong-Wook Seo[3], MD; Dae-Won Sohn, MD[1]

[1]Department of Internal Medicine, Cardiovascular center,

[2] Department of internal Medicine, Division of Endocrinology and Metabolism

[3]Department of Pathology.

Seoul National University College of Medicine,

Seoul National University Hospital. Seoul, Korea

Running Title: Effect of Sildenafil on Mitral Regurgitation

Address for correspondence:

Yong-Jin Kim, MD, PhD

Department of Internal Medicine, Seoul National University Hospital College of Medicine,

Cardiovascular Center, Seoul National University Hospital, Seoul, Korea.

28 Yongon-dong, Chongno-gu, Seoul, 110-744, Korea

Tel: (82)(2) 2072-1963, Fax: (82)(2) 2072-2577, E-mail: kimdamas@snu.ac.kr

Detailed Methodology

Surgical procedure and some concerns for mitral regurgitation creation

The rats were anesthetized with 3% isoflurane at a rate of 4L/min oxygen and then they were intubated with a blunt 16-gauge needle, followed by mechanical ventilation with the M-683 (Harvard Apparatus Inc., MA, U.S.A) under 2-3% isoflurane in a mixture of 50% O_2. Body temperature was maintained at 37'C by placing the rats on a heating pad during the procedure. After successful anesthesia, intracardiac echocardiographic catheter (AcuNav™, Acuson/Siemens Corp, Mountain View, CA) was inserted into the esophagus for transesophageal echocardiography. A lateral thoracotomy was performed and the pericardium was opened. To locate the insertion site of the puncture needle accurately, the LV was gently pressed with a clean cotton swap. A needle (23 gauge, 0.5 mm external diameter) was inserted into the LV via apical puncture and was advanced toward the mitral valve to make a hole in the leaflet and create MR under the guidance of transesophageal echocardiography (supplementary Fig. 1). MR was considered significant if a regurgitant jet area occupied more than 45% of the left atrium (LA). The sham group underwent the same procedure but without damaging the mitral valve. All rats were given 2 ml subcutaneous injection of isotonic saline, meloxicam (Boehringer Ingelheim, Germany 0.4mg/g s.c.) postoperatively and also, cefazolin (50mcg/g i.m.) for preventing infection 2 times a day for 2 days.

In the establishment of our animal model, we focused on several aspects to make it useful for future experiments. Our first concern was the heart size and gender that have been neglected in some of the previous experiments. In our pilot study, we found that rats showed a rapid growth of the heart between 8 and 10 weeks of age (LVESD; 3.40± 0.15mm vs 4.02± 0.27mm, LVEDD; 6.41±0.34mm vs 7.31±0.34mm for 8 vs 10 weeks of age, $p < 0.01$) and thus this period was not optimal for the evaluation of LV remodeling. Therefore, in this study,

we used only male rats at the age of 10 weeks. Second, we had to determine adequate severity of MR to induce substantial LV remodeling without excessive mortality in acute phase. We found that 23G needle with external diameter of 0.5 mm was the best for the purpose. At the postmortem study, the mean area of the hole was 0.79 ± 0.34 mm^2. Obviously, a "learning curve" was noted in our experience. In our first pilot study, the MR operation was successful only three out of nine (33%) rats. It took 4 months for the consistent technique for MR formation in this study. Interestingly, the hole of mitral leaflet spontaneously regressed in some of the animals of our pilot study. Thus, serial echocardiographic confirmation of MR and direct visualization of the hole at the harvest time were important.

In our animal model of MR, acute stage was defined from MR creation to the 2^{nd} week after MR. We observed slight increase of LV diastolic dimension without change of systolic dimension and thus hyperdynamic LV systolic function. In this stage, LV wall thinning occurred as LV began to dilate. Chronic compensated stage could be defined from the 3^{rd} week to around the 14^{th} week. In this stage, LV diastolic and systolic volume increased constantly. Though remained in the normal range, LVEF became significantly lower in MR group from the 12^{th} week with systolic dimension dilatation. The decompensation seemed to begin after the 14^{th} week and became evident between the 20^{th} and 26^{th} week when the mortality dramatically increased. So we decided to analyse microarray before decompensation phase.

Surgical Procedure for Hemodynamic Monitoring

The rats were anesthetized with isoflurane inhalation and placed in the supine position on a heat pad with a rectal probe connected to a thermoregulator and ventilated. The right internal jugular vein was cannulated for fluid administration. After anterior thoracotomy, the microtip PV catheter (SPR-838, Millar Instruments, US) was introduced into the LV cavity via the

apical approach along the longitudinal axis of the heart until stable PV loops were obtained[1, 2]. PV loops were acquired with the ventilator off for 5-10 seconds after 10 minutes of stabilization. The sampling rate was 1,000/s using the ARIA PV conductance system (Millar Instruments) coupled to a PowerLab/4SP A/D converter (AD Instruments; Mountain View, CA, USA) and a personal computer. To get Vo, additional loops were acquired during injection of 500µl of 15% hypertonic saline. Ten to twenty successive cardiac cycles were obtained. True volumes were calculated with correction based on the EF of echocardiography and saline calibrations as described previously [3, 4]. Analyses of the loops were performed using a commercially available cardiac PV analysis program, PVAN 3.5 (Millar Instruments). Heart rate, maximal LV systolic pressure, LV end-diastolic pressure (EDP), mean arterial pressure, maximal slope of systolic pressure increment (+dP/dt) and diastolic pressure decrement (-dP/dt), time constant of LV pressure decay (τ), stroke volume (SV) and end-systolic/diastolic volume (ESV/EDV) were calculated. Additionally, end-systolic pressure volume relation (ESPVR), SW-EDV relation [preload recruitable stroke work (PRSW)], dP/dt_{max}-EDV relation, and end-diastolic PV relation (EDPVR) were measured by transient occlusion of the inferior vena cava with a silk snare suture.

Immunohistochemical Analysis

Mid ventricle were removed for histopathology and were preserved in 4% paraformaldehyde and embedded in paraffin. The tissue was sectioned into 4 µm sections, stained with Masson's trichrome for evaluation of the degree of fibrosis and with picrosirius red for measurement of collagen deposition. Quantitative measurement of the area of perivascular fibrosis was calculated as the ratio of the area of fibrosis surrounding the vessel wall to the total vessel area using NIH image analysis software (Image J ver. 1.38, National Institutes of Health) [5]. At least 10 arterial cross sections were examined per field. Apoptosis

was assessed using the Terminal deoxynucleotidyl transferase-mediated UTP nick-end labeling (TUNEL) technique (DNA fragmentation, Oncor, Gaithersburg, MD). The detailed protocol was previously published [6]. To quantify apoptosis, TUNEL-positive cells in 10 fields for each section was quantitatively evaluated as a percent of that of total cells at a magnification of 400X in a blind manner

Microarray analysis

For control and test RNAs, the synthesis of target cRNA probes and hybridization were performed using Agilent's Low RNA Input Linear Amplification kit (Agilent Technology, USA) according to the manufacturer's instructions. The hybridized images were scanned using Agilent's DNA microarray scanner and quantified with Feature Extraction Software (Agilent Technology, Palo Alto, CA). All data normalization and selection of fold-changed genes were performed using Gene SpringGX 7.3 (Agilent Technology, USA). The averages of normalized ratios were calculated by dividing the average of normalized signal channel intensity by the average of normalized control channel intensity.

Functional annotation of genes was performed according to Gene Ontology™ Consortium(http://www.geneontology.org/index.shtml) by GeneSpringGX 7.3. Gene classification was based on searches done by BioCarta (http://www.biocarta.com/), GenMAPP (http://www.genmapp.org/), DAVID (http://david.abcc.ncifcrf.gov/), and Medline databases (http://www.ncbi.nlm.nih.gov/).

References

1. Chang S, Kim Y, Lee H, Kim D, Kim H, Chang H, Sohn D, Oh B, Park Y. Effect of rosuvastatin on cardiac remodeling, function, and progression to heart failure in hypertensive heart with established left ventricular hypertrophy. *Hypertension*. 2009;54:591
2. Pacher P, Nagayama T, Mukhopadhyay P, Batkai S, Kass D. Measurement of cardiac function using pressure-volume conductance catheter technique in mice and rats. *Nature protocols*. 2008;3:1422-1434
3. Burkhoff D, Mirsky I, Suga H. Assessment of systolic and diastolic ventricular properties via pressure-volume analysis: A guide for clinical, translational, and basic researchers. *American Journal of Physiology- Heart and Circulatory Physiology*. 2005;289:H501
4. Lips D, vd Nagel T, Steendijk P, Palmen M, Janssen B, v. Dantzig J, De Windt L, Doevendans P. Left ventricular pressure-volume measurements in mice: Comparison of closed-chest versus open-chest approach. *Basic research in cardiology*. 2004;99:351-359
5. Ichihara S, Senbonmatsu T, Price Jr E, Ichiki T, Gaffney F, Inagami T. Angiotensin ii type 2 receptor is essential for left ventricular hypertrophy and cardiac fibrosis in chronic angiotensin ii-induced hypertension. *Circulation*. 2001;104:346
6. Loo D. In situ detection of apoptosis by the tunel assay: An overview of techniques. *DNA Damage Detection In Situ, Ex Vivo, and In Vivo: Methods and Protocols*. 2011
7. Mokni W, Keravis T, Etienne-Selloum N, Walter A, Kane MO, Schini-Kerth VB, Lugnier C. Concerted regulation of cgmp and camp phosphodiesterases in early cardiac hypertrophy induced by angiotensin ii. *PloS one*. 2010;5:e14227
8. Francis SH, Turko IV, Corbin JD. Cyclic nucleotide phosphodiesterases: Relating structure and function. *Progress in nucleic acid research and molecular biology*. 2000;65:1-52

Supplementary figure legends

Supplementary figure 1.

Surgical procedures of making mitral regurgitation (MR)

A. Lateral thoracotomy was performed on the left side of the sternum through the 3rd or 4^{th} intercostal space and a needle was inserted.

B. Advancing a needle toward mitral valve leaflet; Red arrow indicates the needle.

C. Severe MR was detected by color Doppler after MR procedure

D. The MR jet and LA area were measured 1 week after MR development by transthoracic echocardiography.

Supplementary figure 2.

Mean body weight among three groups. The mean weight gain of the MR and MR+SIL rats during the 16 weeks period tended to lag behind the sham rats without statistical significance.

Supplementary figure 3

Heat map of the 448 genes were expressed by at least 1.5-fold in MR rats including 197 upregulated (A) and 251 downregulated (B) genes compared with sham and MR+SIL. Red indicates upregulation; black, no change; green, downregulation vs baseline with scale of color corresponding to fold change.

Supplementary figure 1.

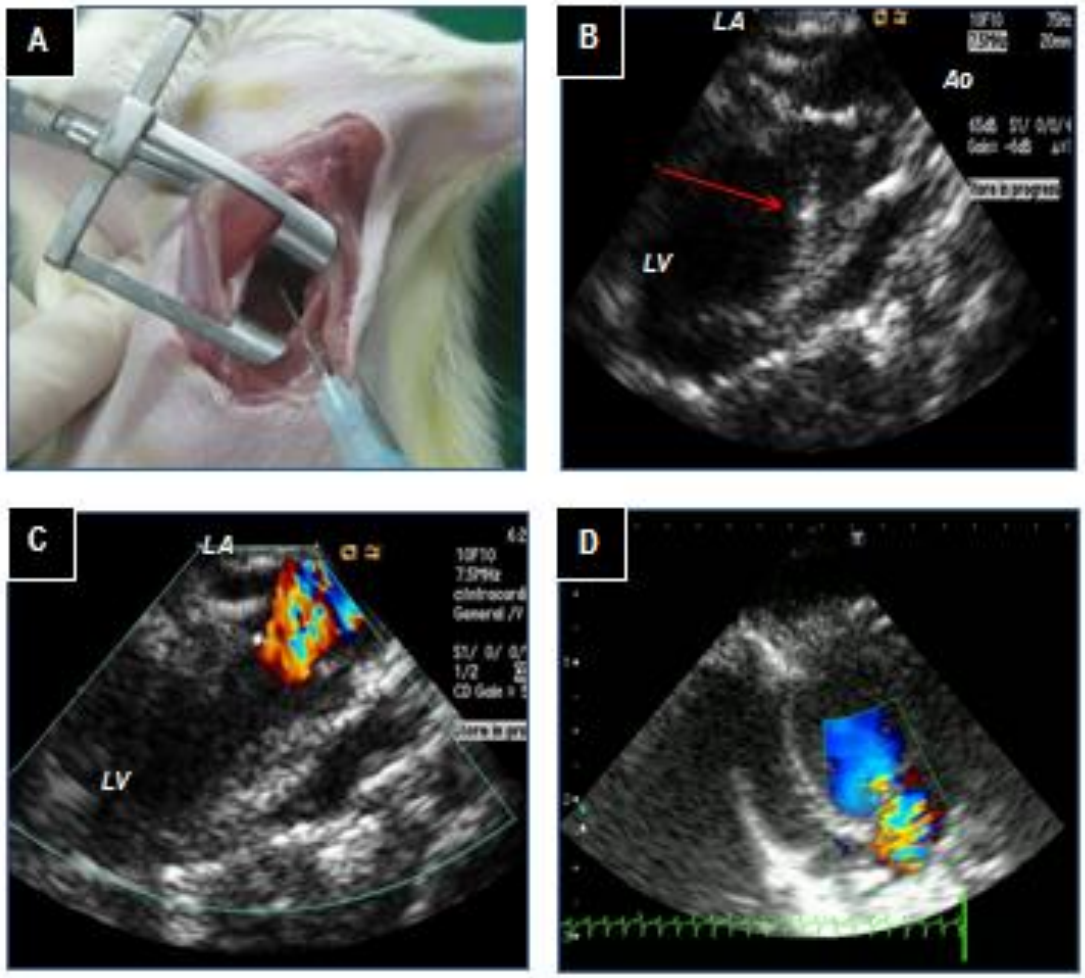

Supplementary figure 2.

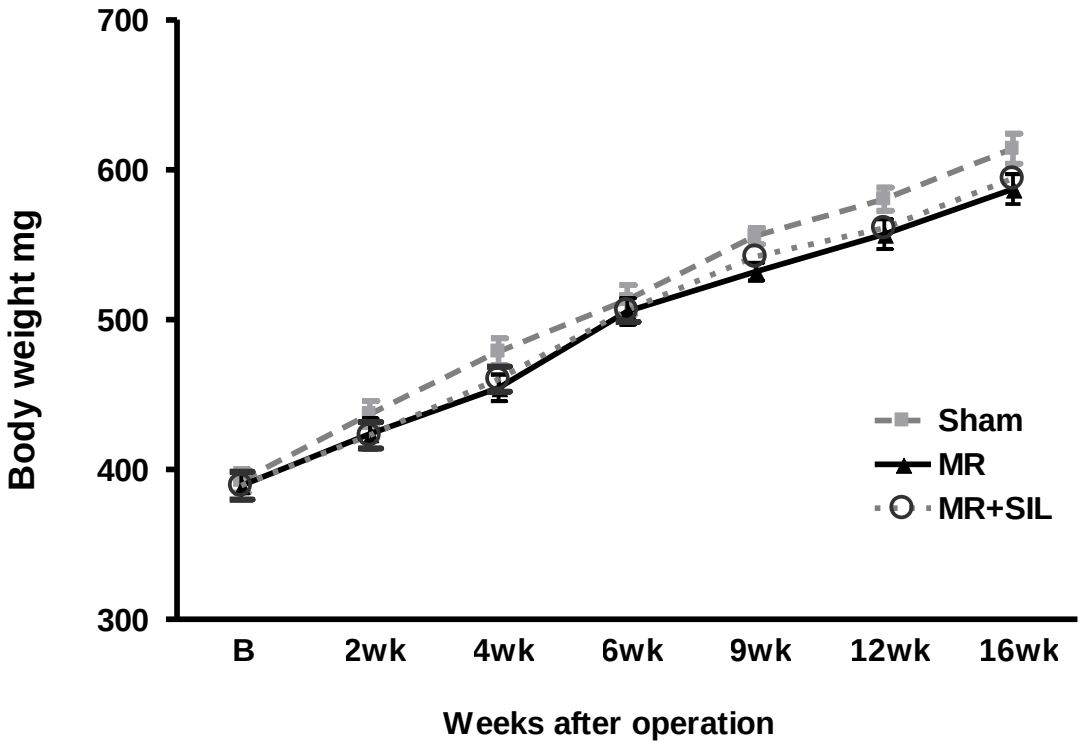

Supplementary figure 3.

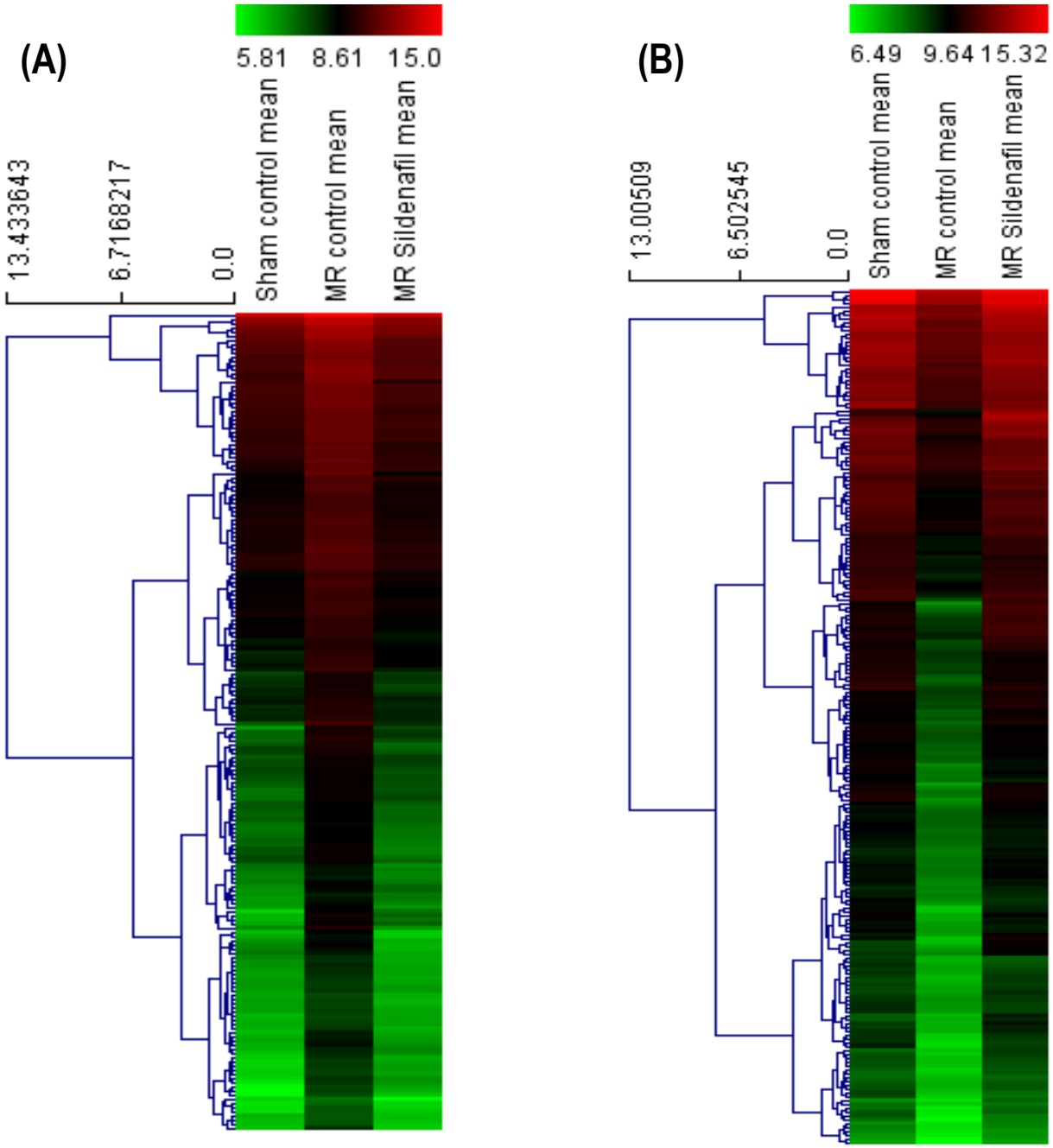

Supplementary table 1.

The List of Gene Sets with Significant Enrichment Scores (ES, P<0.01).

			Sham vs. MR			MR vs. MR+SIL	
Gene Set	Class	Genes (No)	ES	p value	Size	ES	p value
GPCRPATHWAY	C2	23	-0.68255293	0	23	0.52691597	0
GNF2_CD33	C4	20	-0.64632237	0	20	0.47325414	0
UVB_NHEK4_6HRS_UP	C2	16	-0.6422942	0	16	0.5843142	0
CROONQUIST_IL6_RAS_UP	C2	15	-0.62075895	0	15	0.61317587	0
GNF2_FOS	C4	16	-0.59804004	0	16	0.49633634	0
CROONQUIST_IL6_STROMA_UP	C2	21	-0.597425	0	21	0.42403877	0
CCR5PATHWAY	C2	18	-0.59632444	0	18	0.43007636	0
CMV_8HRS_UP	C2	16	-0.59034806	0	16	0.4945651	0
IL6PATHWAY	C2	18	-0.58482593	0	18	0.528253	0
G1_S_TRANSITION_OF_MITOTIC_CELL_CYCLE	C5	15	-0.5819848	0	15	0.5915283	0
GNF2_IGFBP1	C4	17	-0.58028936	0	17	0.5894931	0
MODULE_382	C4	22	-0.5734105	0	22	0.66842264	0
CROONQUIST_RAS_STROMA_UP	C2	15	-0.57083976	0	15	0.54528844	0
CDMACPATHWAY	C2	15	-0.56861526	0	15	0.5073269	0
LEE_TCELLS3_UP	C2	24	-0.55996156	0	24	0.413297	0
CCR3PATHWAY	C2	20	-0.55321383	0	20	0.41676757	0
CXCR4PATHWAY	C2	21	-0.55279344	0	21	0.48638755	0
LINDSTEDT_DEND_8H_VS_48H_UP	C2	39	-0.55110425	0	39	0.43290132	0
ADIP_DIFF_CLUSTER3	C2	17	-0.5455381	0	17	0.6032467	0
SPPAPATHWAY	C2	21	-0.54538107	0	21	0.49615264	0
AT1RPATHWAY	C2	28	-0.5436344	0	28	0.5075726	0
MODULE_367	C4	26	-0.538402	0	26	0.38241568	0
PASSERINI_INFLAMMATION	C2	17	-0.53667206	0	17	0.58285594	0
BCRPATHWAY	C2	26	-0.52640563	0	26	0.41382107	0
REGULATION_OF_PROTEIN_MODIFICATION_PROCESS	C5	20	-0.52350223	0	20	0.54774433	0
VIPPATHWAY	C2	18	-0.5203666	0	18	0.4019881	0
POSITIVE_REGULATION_OF_CELL_DIFFERENTIATION	C5	15	-0.51972675	0	15	0.35104468	0
JISON_SICKLE_CELL	C2	23	-0.5163545	0	23	0.40098867	0
ZHAN_MM_MOLECULAR_CLASSI_DN	C2	17	-0.51632905	0	17	0.57981193	0
FALT_BCLL_IG_MUTATED_VS_WT_UP	C2	20	-0.51562107	0	20	0.4589497	0
GCM_PTK2	C4	40	-0.5118762	0	40	0.45367202	0
LIZUKA_G2_GR_G3	C2	15	-0.51087797	0	15	0.6560526	0
STRESS_TPA_SPECIFIC_UP	C2	20	-0.5086299	0	20	0.3734148	0
GNF2_TAL1	C4	26	-0.50839764	0	26	0.5728936	0

DORSAM_HOXA9_DN	C2	17	-0.50828165	0	17	0.39426166	0
GNF2_CDC27	C4	22	-0.50595254	0	22	0.5798319	0
PASSERINI_ADHESION	C2	22	-0.50546247	0	22	0.6577618	0
IFN_GAMMA_UP	C2	20	-0.5050956	0	20	0.4674851	0
EDG1PATHWAY	C2	21	-0.5024325	0	21	0.69462144	0
PASSERINI_GROWTH	C2	30	-0.49091655	0	30	0.35128912	0
GNF2_ANK1	C4	25	-0.4860897	0	25	0.5278036	0
GNF2_SPTB	C4	25	-0.4860897	0	25	0.5278036	0
GNF2_SPTA1	C4	27	-0.48427492	0	27	0.5802883	0
FMLPPATHWAY	C2	26	-0.48140424	0	26	0.54253864	0
PYK2PATHWAY	C2	25	-0.47761953	0	25	0.4634575	0
ERKPATHWAY	C2	23	-0.47752348	0	23	0.38381964	0
CELL_GROWTH_AND_OR_MAINTENANCE	C2	31	-0.47659698	0	31	0.38383582	0
GNF2_TIMP2	C4	20	-0.47557914	0	20	0.563822	0
ET743_SARCOMA_72HRS_UP	C2	34	-0.47404426	0	34	0.4710121	0
MODULE_108	C4	35	-0.47253314	0	35	0.52990705	0
GNF2_KISS1	C4	19	-0.47211227	0	19	0.5798732	0
BRCA1KO_MEF_DN	C2	37	-0.46840483	0	37	0.37944198	0
ZHAN_MULTIPLE_MYELOMA_VS_NORMAL_DN	C2	24	-0.46543878	0	24	0.49981317	0
GILDEA_BLADDER_UP	C2	15	-0.45915794	0	15	0.4450995	0
INSULINPATHWAY	C2	17	-0.45906976	0	17	0.36727202	0
STEROID_BIOSYNTHETIC_PROCESS	C5	16	-0.45698878	0	16	0.4077422	0
MODULE_418	C4	25	-0.45637232	0	25	0.4089294	0
MODULE_322	C4	28	-0.4560361	0	28	0.47139147	0
MODULE_362	C4	16	-0.45470858	0	16	0.4289022	0
RHYTHMIC_PROCESS	C5	18	-0.45430204	0	18	0.43919545	0
GNF2_MMP11	C4	16	-0.44851413	0	16	0.610244	0
ROSS_CBF_MYH	C2	23	-0.44663757	0	23	0.58098453	0
HALMOS_CEBP_UP	C2	29	-0.44433838	0	29	0.40851527	0
HINATA_NFKB_UP	C2	64	-0.4395395	0	64	0.48163795	0
FETAL_LIVER_ENRICHED_TRANSCRIPTION_FACTORS	C2	29	-0.43891904	0	29	0.42875883	0
CELL_ADHESION_RECEPTOR_ACTIVITY	C2	22	-0.4363057	0	22	0.43484345	0
GNF2_BNIP3L	C4	24	-0.4359979	0	24	0.5416765	0
YANG_OSTECLASTS_SIG	C2	31	-0.43227735	0	31	0.42077395	0
GNF2_RAD23A	C4	22	-0.42824152	0	22	0.50279856	0
ST_DIFFERENTIATION_PATHWAY_IN_PC12_CELLS	C2	27	-0.42750946	0	27	0.4963255	0
CMV-UV_HCMV_6HRS_UP	C2	55	-0.42720556	0	55	0.38781008	0
INTERPHASE	C5	31	-0.4265289	0	31	0.3912818	0
ROSS_PML_RAR	C2	31	-0.42633754	0	31	0.5502655	0
GNF2_CD1D	C4	21	-0.424542	0	21	0.39505285	0
TAKEDA_NUP8_HOXA9_10D_UP	C2	61	-0.4242422	0	61	0.37216726	0

RESPONSE_TO_NUTRIENT_LEVELS	C5	25	-0.42055058	0	25	0.46068797	0
GNF2_PECAM1	C4	25	-0.420396	0	25	0.37018463	0
CAR_HPX	C4	51	-0.4200604	0	51	0.57094014	0
MODULE_226	C4	17	-0.41917244	0	17	0.35103738	0
HDACI_COLON_SUL16HRS_UP	C2	21	-0.4165574	0	21	0.44852975	0
IDX_TSA_UP_CLUSTER1	C2	15	-0.41382015	0	15	0.48862424	0
RESPONSE_TO_EXTRACELLULAR_STIMULUS	C5	29	-0.41374642	0	29	0.3906259	0
ST_ADRENERGIC	C2	29	-0.41224363	0	29	0.44021443	0
LEE_ACOX1_DN	C2	39	-0.41098782	0	39	0.43525627	0
MODULE_174	C4	51	-0.40879533	0	51	0.3528535	0
FEEDING_BEHAVIOR	C5	19	-0.40753257	0	19	0.49436483	0
MODULE_263	C4	27	-0.4060169	0	27	0.39150825	0
INTERLEUKIN_BINDING	C5	19	-0.402392	0	19	0.38682523	0
EIF4PATHWAY	C2	19	-0.4014743	0	19	0.39073327	0
IGF1PATHWAY	C2	17	-0.39995828	0	17	0.3651653	0
GNF2_MAP2K3	C4	26	-0.3958451	0	26	0.44645998	0
RUIZ_TENASCIN_TARGETS	C2	43	-0.39430535	0	43	0.38844472	0
MODULE_440	C4	16	-0.39379758	0	16	0.41904488	0
CHEMOKINE_ACTIVITY	C5	18	-0.39203185	0	18	0.45625585	0
CHEMOKINE_RECEPTOR_BINDING	C5	18	-0.39203185	0	18	0.45625585	0
METPATHWAY	C2	27	-0.38755685	0	27	0.3587055	0
REGULATION_OF_PHOSPHORYLATION	C5	29	-0.38364542	0	29	0.45200315	0
ST_ERK1_ERK2_MAPK_PATHWAY	C2	20	-0.37316942	0	20	0.3629946	0
ZHAN_MM_CD138_MF_VS_REST	C2	16	-0.37267223	0	16	0.4182984	0
HEMATOPOESIS_RELATED_TRANSCRIPTION_FACTORS	C2	51	-0.37198797	0	51	0.3554443	0
GALINDO_ACT_UP	C2	48	-0.3710842	0	48	0.35142434	0
G_PROTEIN_COUPLED_RECEPTOR_BINDING	C5	24	-0.36708376	0	24	0.45865744	0
HOGERKORP_ANTI_CD44_UP	C2	16	-0.36396125	0	16	0.446282	0
TELPATHWAY	C2	16	-0.36230457	0	16	0.39587778	0
VERHAAK_AML_NPM1_MUT_VS_WT_UP	C2	90	-0.36121643	0	90	0.3680169	0
HSA04920_ADIPOCYTOKINE_SIGNALING_PATHWAY	C2	54	-0.36032555	0	54	0.41671214	0
TAKEDA_NUP8_HOXA9_8D_UP	C2	56	-0.35908818	0	56	0.4329368	0
IFN_ANY_UP	C2	40	-0.35855725	0	40	0.36113158	0
BRENTANI_CELL_ADHESION	C2	61	-0.35706916	0	61	0.35144362	0
H2O2_CSBRESCUED_C1_UP	C2	23	-0.3537327	0	23	0.36836156	0
LEE_CIP_DN	C2	45	-0.3533668	0	45	0.47496936	0
ENDOPLASMIC_RETICULUM_PART	C5	32	-0.3528851	0	32	0.37715906	0
ST_JNK_MAPK_PATHWAY	C2	19	-0.35170564	0	19	0.42782012	0
HTERT_DN	C2	30	-0.35148805	0	30	0.4636676	0